


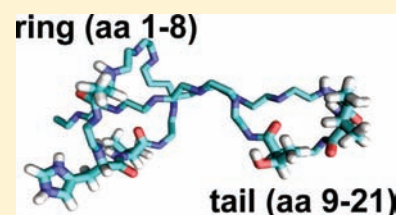
# Sequence Diversity in the Lasso Peptide Framework: Discovery of Functional Microcin J25 Variants with Multiple Amino Acid Substitutions

Si Jia Pan<sup>†</sup> and A. James Link<sup>\*,†,‡</sup>

Departments of <sup>†</sup>Chemical and Biological Engineering and <sup>‡</sup>Molecular Biology, Princeton University, Princeton, New Jersey 08544, United States

 Supporting Information

**ABSTRACT:** Microcin J25 (MccJ25) is a ribosomally synthesized antimicrobial peptide that has an unusual threaded lasso structure in which the C-terminal “tail” of the peptide is fed through a macrocyclic “ring” formed by the N-terminal residues. Production of MccJ25 in *Escherichia coli* is dependent upon a four-gene cluster encoding the structural gene *mcjA*, two maturation enzymes *mcjB* and *mcjC*, and an immunity factor, *mcjD*, in the form of an MccJ25 export pump. Here we have developed a system for orthogonal control of the expression of *mcjA* and *mcjD*, thus permitting independent control of MccJ25 production and export/immunity in *E. coli*. We used this system to screen saturation mutagenesis libraries targeted to either the ring or tail portions of MccJ25 and discovered nearly 100 new MccJ25 variants that retain antimicrobial function. While multiple amino acid substitutions in the tail portion of the peptide are well-tolerated, mutagenesis of the ring portion of the peptide is detrimental to the antimicrobial function of MccJ25. We demonstrated that the decreased function of the ring variants is due to the inability of these variants to be transported to the cytoplasm of susceptible strains. Additionally, we found several MccJ25 variants from the tail library with improved efficacy toward the MccJ25-sensitive strains *E. coli* and *Salmonella enterica* serovar Newport with the best variants exhibiting a nearly 5-fold increase in potency. The results described here provide further evidence that diverse amino acid sequences can be tolerated by the rigid lasso peptide fold.



## INTRODUCTION

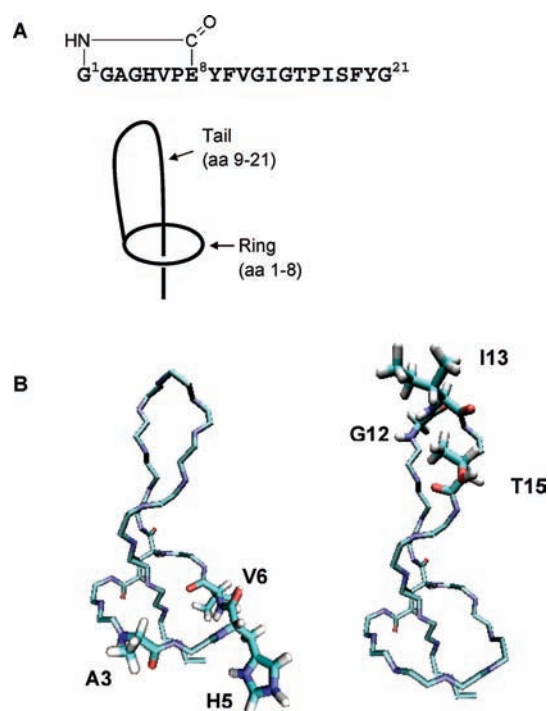
Microcin J25 (MccJ25) belongs to the class of low molecular mass antibacterial peptides termed microcins, secreted by Enterobacteriaceae and active against closely related bacterial species. Microcins are synthesized ribosomally and display miscellaneous post-translational modifications and modes of killing.<sup>1–5</sup> Microcin J25 is 21 amino acids (aa) long and is unique among the microcins in that it has a remarkable threaded lasso topology. An N-terminal ring is formed via an isopeptide bond between the N-terminus of the peptide and a glutamic acid residue at position 8. A tail formed by the 13 C-terminal aa loops back forming a  $\beta$ -hairpin composed of residues 10–16 and threads through the ring (Figure 1A). The tail is locked into place within the ring due to the presence of Phe-19 and Tyr-20 on opposite sides of the ring.<sup>6–8</sup> The lasso structure endows MccJ25 with exceptional stability toward thermal and chemical denaturation as well as resistance to most proteases.<sup>9</sup> Because of this tremendous stability, MccJ25 and other lasso peptides<sup>10–13</sup> have received attention as a potential scaffold for therapeutic peptides.<sup>14</sup> An important step toward the therapeutic applicability of these molecules is the demonstration of the ability to program an arbitrary sequence into the lasso scaffold. Recently, a mutational scanning analysis of MccJ25 was performed by Pavlova et al.<sup>15</sup> in which a nearly complete set of single aa variants of MccJ25 was tested for production and bacterial growth inhibition. Knappe et al. also characterized many single aa variants of the lasso peptide capistruiin.<sup>13</sup> Our group recently published a study on the computational design of

MccJ25 in which we found that several MccJ25 variants containing three aa substitutions retained the lasso structure and some antimicrobial function.<sup>16</sup> Collectively, these previous studies demonstrate that the lasso peptide topology can be reprogrammed, even with multiple aa substitutions. MccJ25 is an ideal peptide for studies of the tolerance of aa substitutions within the lasso scaffold since it has a readily assayable antimicrobial activity that can function as a proxy for lasso peptide formation.

MccJ25 exerts its primary mode of action in susceptible bacteria by inhibiting RNA polymerase (RNAP).<sup>17</sup> It binds to the RNAP secondary channel, interfering with NTP uptake and inhibiting transcription.<sup>18–20</sup> A second, independent mode of action, disruption of the membrane potential leading to inhibition of oxygen consumption and superoxide overproduction, has been demonstrated.<sup>21,22</sup> The antibacterial action of MccJ25 is dependent on its transport into the cell through both the outer-membrane protein FhuA and the inner-membrane protein SbmA.<sup>23,24</sup> The structure–activity relationship of MccJ25 has been probed by several studies. It was suggested that the ring region and the  $\beta$ -hairpin loop formed by the tail play distinct roles in the peptide’s antimicrobial activity. Specifically, the  $\beta$ -hairpin formed by residues 10–16 was found to be crucial in the import of MccJ25 through FhuA but not for RNAP and respiration inhibition.<sup>25–29</sup> This was demonstrated using a thermolysin-digested MccJ25 which is cleaved between residues 10 and 11.<sup>29</sup> The roles played by specific

Received: December 6, 2010

Published: March 10, 2011



**Figure 1.** Representation of the threaded lasso structure of MccJ25. (A) A backbone–side chain lactam linkage between the residues Gly1 and Glu8 of MccJ25 leads to a small cyclized ring (aa 1–8) followed by a C-terminal linear tail (aa 9–13). The C-terminal tail forms a  $\beta$ -hairpin loop and passes back through the ring. (B) The NMR structure of MccJ25 drawn from PDB File 1Q71. Left: The side chains of residues mutagenized in this study in the ring region (A3, H5, V6) are shown. Right: Residues mutagenized in the tail library in this study (G12, I13, T15) are shown.

residues in the peptide have also been reported. The C-terminal glycine was found to be important for RNAP inhibition<sup>30</sup> while site-specific mutation of His-5 demonstrated that this residue was important for recognition by the inner membrane receptor SbmA.<sup>31</sup>

The biosynthesis of MccJ25 is specified by the structural gene *mcjA* encoding the MccJ25 precursor and the genes *mcjB* and *mcjC* encoding the maturation enzymes involved in post-translational modification of MccJ25. The *mcjD* gene product is an ATP-binding cassette (ABC) transporter responsible for immunity. These four genes were found naturally in a plasmid-borne gene cluster.<sup>32,33</sup> The gene product of *mcjA* is a 58 aa linear precursor, the N-terminal 37 aa of which forms a leader peptide. During maturation, the leader peptide is removed and the mature lasso peptide is formed via the enzymatic activities of MccJ25 and MccJ26. To create a robust platform for the study of MccJ25, we have previously engineered gene clusters with orthogonal control of the *mcjA* structural gene and the maturation/export operon *mcjBCD*.<sup>34</sup> Here, we build upon this work by constructing a MccJ25 expression system in which production (*mcjA* expression) and export (*mcjD* expression) of MccJ25 are orthogonally regulable. We have utilized this system in a high-throughput screen of saturation mutagenesis libraries of the ring and  $\beta$ -hairpin tail regions of MccJ25 for antibacterial activity and discovered 93 new functional MccJ25 variants containing up to three aa substitutions. Of these new variants, a dozen exhibited improved antimicrobial efficacy against susceptible *Escherichia coli* and *Salmonella* strains. The results here further demonstrate that the lasso scaffold of MccJ25 is very tolerant to aa substitutions and provide new insights to the structure–activity relationship of MccJ25.

## MATERIALS AND METHODS

**Media and Bacterial Strains.** The *E. coli* strain XL-1 Blue [recA1, endA1, gyrA96, thi, hsdR17, supE44, relA1, lac, (F' proAB, lacI<sup>q</sup>, lacZ $\Delta$ M15, Tn10 (tetR))] was used in this study for all recombinant DNA work and MccJ25 production. The *E. coli* strain DH5 $\alpha$  and *Salmonella enterica* sp. *enterica* serovar Newport, colloquially known as *Salmonella newport*, were used in antimicrobial susceptibility tests. Bacterial cells were grown in LB broth at 37 °C with shaking. Antibiotics were added to a final concentration of 100  $\mu$ g/mL for ampicillin and 25  $\mu$ g/mL for chloramphenicol. Bacterial cultures were induced with 0.2% arabinose and 1 mM IPTG as needed. M63 minimal medium was composed of 2 g/L (NH<sub>4</sub>)<sub>2</sub>SO<sub>4</sub>, 13.6 g/L KH<sub>2</sub>PO<sub>4</sub>, adjusted to pH 7 with KOH. M63 medium was supplemented with 0.2% glucose, 1 mM MgSO<sub>4</sub>, and 0.5  $\mu$ g/mL thiamine. A solution of 20 amino acids was added to a final concentration of 40 mg/L of each aa to the M63 soft agar.

**Plasmid and Library Construction.** The plasmids and primers used in this study are listed in Supplementary Table 1. The *mcjD* gene fragment was amplified from plasmid pTUC202<sup>35,36</sup> by PCR using upstream primer “*mcjD* F” and downstream primer “*mcjD* R”. The *mcjD* fragment was then digested with *Kpn*I and *Hind*III and inserted into *Kpn*I–*Hind*III digested pBAD33,<sup>37</sup> producing pBAD33-*mcjD* (pJP31, Figure 2A). The plasmid pWC8 was constructed by first generating pQE80-*mcjA*, then adding the *mcjBC* operon. The vector pQE80 (Qiagen) and pJP3 carrying the MccJ25 engineered gene cluster described previously<sup>34</sup> were both digested with *Eco*RI and *Hind*III. The *Eco*RI–*Hind*III fragment containing *mcjA* from pJP3 was inserted into similarly digested pQE80 to generate pQE80-*mcjA*. The *mcjBC* genes were amplified from pTUC202 using upstream primer “*mcjBC* F” and downstream primer “*mcjBC* R”. The amplified *mcjBC* fragment was digested with *Nhe*I and ligated into similarly digested pQE80-*mcjA*, generating pWC8 (Figure 2A).

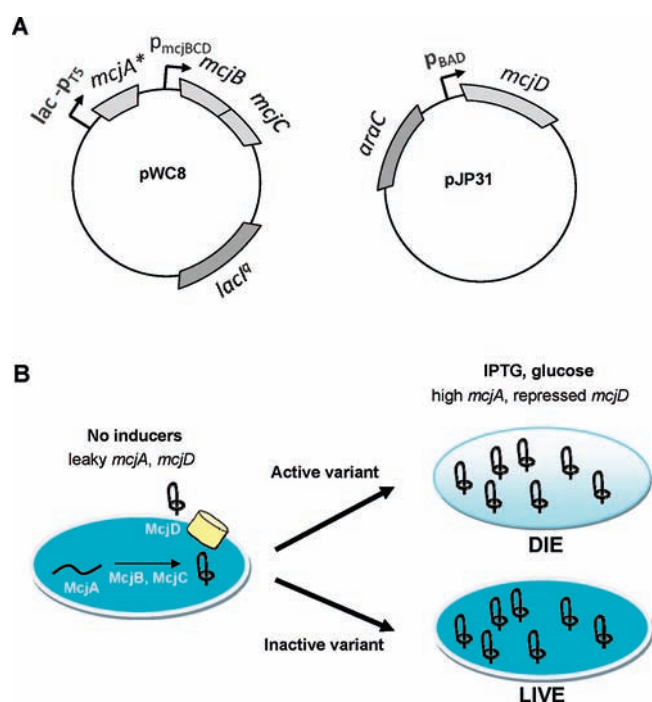
To construct the NNT saturation mutagenesis library of *mcjA* mutants, the “*mcjA* ring F” and “*mcjA* ring R” oligonucleotides were used to synthesize the mature peptide coding region of *mcjA* ring mutants by primer overlap PCR, and likewise the “*mcjA* tail F” and “*mcjA* tail R” oligonucleotides were used to synthesize the mature peptide region of the *mcjA* tail mutants. The fragment coding for the signal peptide of *mcjA* and its upstream region extending to the *Xho*I site from pJP3 was amplified using upstream primer “*mcjA* signal F” and downstream primer “*mcjA* signal R”. Next, the fragment containing the *mcjA* signal and the mature peptide coding fragment of *mcjA* mutants were joined using assembly PCR to make full-length mutant *mcjA*. Both the ring and tail mutant *mcjA* fragments were digested with *Xho*I and *Hind*III, and pWC8 was digested with *Xho*I and *Hind*III to remove wild type *mcjA*, then the mutant *mcjA* fragments were ligated into the place of wild type *mcjA* in the pWC8 plasmid, creating the *mcjA* ring and tail NNT libraries.

**Library Transformation.** For the ring and tail libraries, plasmids carrying the libraries were transformed into XL-1 Blue cells and the cells were spread onto LB plates. About 12 000 colonies were obtained for each library, and the colonies were scraped from the plates and grown in 100 mL of fresh LB broth for an hour. Plasmids carrying the libraries were extracted from the culture by midiprep (Qiagen Plasmid Midi Kit), and subsequently used to transform cells containing pJP31 for library screening.

For the tail arabinose (tail ara+) library, plasmids carrying the tail library were transformed into *E. coli* cells containing pJP31. The cells were spread onto LB plates containing 0.2% arabinose. About 20 000 colonies were obtained and harvested by scraping and grown in 100 mL of LB broth supplemented with arabinose for an hour. Aliquots of the culture containing the library were mixed with equal parts of a 65% glycerol solution and frozen at –80 °C until needed for screening.

**Replica Plating Assay for Identification of Intracellularly Functional MccJ25 Variants.** XL-1 Blue cells harboring the *mcjA* ring and tail libraries prepared as described above were grown on LB plates (25 g/L agar) overnight. The colonies on each plate were transferred onto two fresh plates (25 g/L agar) by replica plating.





**Figure 2.** An orthogonally regulable system for MccJ25 production and export. (A) Illustration of the two plasmids used in the orthogonally inducible system. The plasmid pWC8 is derived from the pQE80 vector, carrying mutant *mcjA* genes (*mcjA\**) under the control of an IPTG-inducible promoter and *mcjB* and *mcjC* under the control of their natural constitutive promoter. The plasmid pJP31 is a pBAD33-based plasmid carrying the *mcjD* gene under the control of an arabinose-inducible promoter. (B) Schematic of the orthogonally inducible system for MccJ25 derivative production. The genes *mcjA* and *mcjD* are independently inducible (by IPTG and arabinose, respectively) while *mcjB* and *mcjC* are constitutively expressed in *E. coli* cells. In the noninduced state, leaky expression causes low levels of both McjA and the export pump McjD to be produced (left). When IPTG and glucose are added, the *mcjA* gene is induced and the *mcjD* gene is repressed leading to cytoplasmic levels of McjA that exceed the capability of the scarce McjD. If McjA is processed into mature MccJ25 that exhibits antibacterial activity inside the cytoplasm, accumulated MccJ25 will inhibit the growth of the host cell (top right). However, MccJ25 variants that are inactive will have no effect on the cell growth (bottom right).

During replica plating, the Petri dish carrying the original colonies was inverted and lowered onto a block (Scienceware Replica-Plating Tool) covered with velveteen square. After carefully lifting the original plate, an LB plate and subsequently an LB plate with IPTG/glucose were inverted and lowered onto the velveteen to create two plates carrying identical colony replicas. Following overnight incubation of the two replica plates, clones that were growth-inhibited on the IPTG/glucose plate were identified as producers of functional MccJ25 variants.

**MccJ25 Variants Culture Supernatant and Zone of Inhibition Assay.** Clones selected from replica plating were grown in LB medium supplemented with arabinose at inoculation to induce *mcjD* expression. When the culture OD<sub>600</sub> reached 0.4–0.5, IPTG was added to induce mutant *mcjA* expression. About 20 h after induction by IPTG, the culture supernatant was collected by centrifugation and heated at 98 °C for 10 min. To perform the zone of inhibition assay to assess the antimicrobial activity of MccJ25 variants, culture supernatants (5 μL) were spotted on M63 minimal medium plates. After the drops evaporated to dryness, the plates were each overlaid with 5 mL of M63 soft agar (6.5 g/L agar) inoculated with exponentially growing *S. Newport* or LB soft agar (6.5 g/L agar) inoculated with exponentially growing *E. coli* DH5α at 10<sup>7</sup> cells/mL. After solidification, the plates were incubated

overnight at 37 °C and then examined for zones of growth inhibition. The inhibition zone diameters were measured as an initial quantitative estimate of the efficacy of the variants. As a control, supernatant from cells producing wild-type MccJ25 was spotted on each plate, and the diameter of its zone of inhibition was measured.

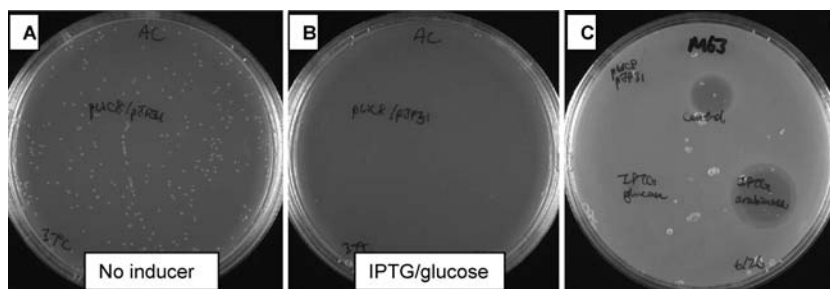
**Quantifying Relative Production Level of MccJ25 Variants by HPLC Analysis.** The method of quantifying relative production level of MccJ25 in a culture has been described previously.<sup>34,38</sup> Briefly, MccJ25 variant supernatants prepared as described above in the culture supernatant section were extracted with 2 vol of *n*-butanol. Following the extraction, 1 mL of the butanolic extract was evaporated to dryness under vacuum and dissolved in 200 μL of water. The sample was then applied to an analytical HPLC column (Zorbax 300SB-C18, 4.6 × 150 mm, Agilent) and eluted by water/0.1% trifluoroacetic acid (A) and acetonitrile/0.1% trifluoroacetic acid (B), with the gradient increasing linearly from 10% to 50% B in 20 min followed by an increase to 90% B in 5 min and holding at 90% B for 5 min. The retention time of wild type MccJ25 was found to be around 16.0 min using these conditions.<sup>34</sup> Hence, we examined the chromatograms of the variants in the area near 16.0 min to determine their retention times. Integrating the area under the peak produced an approximate relative production level of the MccJ25 derivatives.

**Determination of Last Active Dilution of MccJ25 Variants.** Supernatants of cultures producing MccJ25 variants were serially diluted in LB medium. The diluted samples were spotted on plates and overlaid with susceptible bacterial strains as in the zone of inhibition assay described above. Upon examining the plates, the dilution that produced the last zone of growth inhibition was used as a quantitative measure of the relative efficacy of the variants. The dilution analysis was performed in at least triplicate with different biological replicates.

## RESULTS

**Design of MccJ25 Saturation Mutagenesis Libraries.** We created a ring library and a tail library, randomizing the positions A3, H5, V6; and G12, I13, T15, respectively. Figure 1B illustrates the structure of MccJ25 and highlights the location of the substituted residues in each library. These residues were chosen because they correspond to several different locations throughout the peptide. Moreover, these residues all exhibit some permissibility to mutation in the Pavlova et al. study of single aa variants of MccJ25.<sup>15</sup> The NNT codon was chosen to randomize all substitution positions. Representing 16 codons and 15 amino acids, the NNT codon allowed a reduced number of degenerate codons (only Ser is represented more than once) and a greatly decreased theoretical library size compared with the NNK codon commonly used for saturation mutagenesis studies. The 15 aa's included in the library (Phe, Leu, Ile, Val, Ser, Pro, Thr, Ala, Tyr, His, Asn, Asp, Cys, Arg, Gly) are broadly unbiased as they consist of polar and nonpolar, aliphatic and aromatic, and negatively charged and positively charged residues. Both the ring and tail libraries have a theoretical library diversity of 15<sup>3</sup> or 3375 possible protein sequences. This relatively small library size ensures that high coverage of the library can be achieved by screening just thousands of clones.

**Construction and Testing of Orthogonally Inducible MccJ25 Production System.** Our screening method involves controlling separately the state of immunity and MccJ25 production in *E. coli*. This requires an orthogonally inducible system for the expression of mutant precursor McjA and the immunity factor McjD encoding the MccJ25 export pump (Figure 2A). If *mcjD* can be effectively turned off while the mutant *mcjA*, *mcjB*, and *mcjC* genes are turned on, variants that are successfully matured by McjB and McjC into the stable lasso fold will accumulate in the cytoplasm. If a variant possesses the ability to inhibit RNAP or the respiratory chain, it would become toxic at sufficient intracellular concentration. In



**Figure 3.** Characterization of growth of cells harboring the orthogonally inducible MccJ25 production system. (A) *E. coli* XL-1 Blue harboring pWC8 and pJP31 and producing wild-type MccJ25 were able to form colonies after incubation overnight at 37 °C on LB plate with no inducer. (B) The same cells could not grow after overnight incubation at 37 °C on LB plate with IPTG and glucose. (C) Zone of inhibition assay against *S. Newport* to evaluate MccJ25 production using the orthogonally inducible system. Supernatants of *E. coli* XL-1 Blue (pWC8, pJP31) culture grown at 37 °C overnight with no inducer (top), in the presence of IPTG and glucose (left), and in the presence of IPTG and arabinose (right) were spotted on a lawn of *S. Newport*. Growth inhibition zones indicate the presence of MccJ25 in the supernatants.

**Table 1. Library Screening Statistics**

library	ring	tail	tail ara+
Clones screened by replica plating (Stage 1)	4100	3900	4880
Clones selected for zone of inhibition assay (Stage 2)	100	67	247
Active clones against <i>S. Newport</i>	9	57	193
Distinct sequences	8	49	36 <sup>a</sup>
Variants with large (relative zone diameter >0.8) inhibition zone	0	23	43

<sup>a</sup> Only clones exhibiting large inhibition zones from the tail ara+ library were sequenced; sequences that were duplicated or have already appeared in the tail library were not counted.

contrast, variants that cannot be matured or were otherwise inactive will have no effect on cell growth (Figure 2B). By taking advantage of the antimicrobial function of MccJ25, we can quickly distinguish intracellularly active clones from those that are inactive.

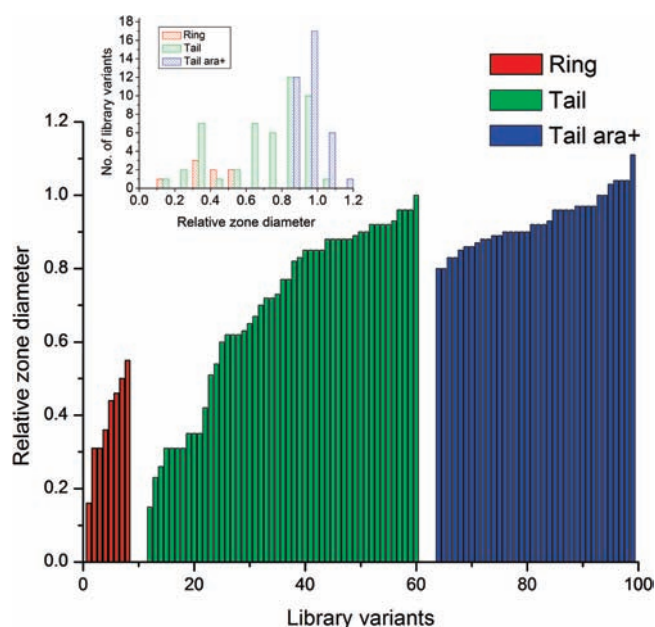
To construct the orthogonally inducible system, we placed *mcjA* under the control of the viral T5 promoter with a double *lac* operator repression module and *mcjD* under the control of the *p<sub>araBAD</sub>* promoter of the arabinose operon. Two plasmids were constructed: pWC8 carrying IPTG-inducible *mcjA*, and an *mcjBC* operon under its natural promoter; and pJP31 carrying arabinose-inducible *mcjD* (Figure 2A). Since the screening method requires tightly regulated expression of the genes, we chose the host vector pQE80, which has a copy of the *lac* repressor *lacI<sup>q</sup>*, to minimize leaky expression of *mcjA*. In addition, we used the *E. coli* strain XL-1 blue, which has an episomal copy of *lacI<sup>q</sup>*, for expression and screening. The gene *mcjD* was cloned into pBAD33,<sup>37</sup> containing the repressor gene *araC* and the arabinose-inducible *p<sub>araBAD</sub>* promoter, which can be turned off rapidly upon withdrawal of arabinose and further repressed in the presence of glucose.<sup>37</sup>

We tested this system by spreading *E. coli* XL-1 Blue cells transformed with pWC8 carrying wild-type *mcjA* and pJP31 onto two plates, one with and one without IPTG/glucose. Upon overnight incubation, we observed that XL-1 Blue cells grew and formed colonies on the plate with no inducer (Figure 3A). At the same time no colonies formed on the plate with IPTG/glucose (Figure 3B), demonstrating that cell growth had been effectively inhibited by the production of wild-type MccJ25 under the *mcjD* repressed condition. The cells were also cultured in liquid media, and supplemented with IPTG/glucose, IPTG/arabinose, or no inducer. Supernatants from these overnight cultures were spotted in a zone of inhibition assay against MccJ25-sensitive *S. Newport* to detect the level of MccJ25 production (Figure 3C).

When no inducer was added to the culture, leaky expression led to some MccJ25 production (labeled as control in Figure 3C). When IPTG and arabinose were added at inoculation, the production level was much higher. However, when IPTG and glucose were added to the culture at inoculation, cell growth was deterred reaching an OD<sub>600</sub> of 0.52 28 h after inoculation, and only a negligible amount of MccJ25 was detectable in the culture supernatant (Figure 3C).

**Screening of the Ring and Tail Libraries for Functional MccJ25 Variants.** The mutant *mcjA* genes produced by saturation mutagenesis were cloned in place of wild-type *mcjA* in the plasmid pWC8. The ring and tail libraries were screened in two stages using the orthogonally inducible MccJ25 production system described above. In stage one, colonies of XL-1 Blue cells harboring pWC8 derivatives and pJP31 on a Petri dish were duplicated onto two fresh plates, one with no inducer and one with IPTG and glucose, by replica plating. After overnight incubation of the two replica plates, clones that produced toxic MccJ25 variants under IPTG induction were unable to grow into a colony. We selected only clones with severe growth inhibition on IPTG/glucose plates for further testing in the second stage of the screen. In stage two, selected clones from stage one were inoculated in LB medium supplemented with arabinose and induced with IPTG during midexponential growth. The supernatants were then tested by the zone of inhibition assay against *S. Newport* and *E. coli* DHS $\alpha$  to evaluate the antimicrobial activity of these variants.

We screened 4100 clones from the ring library and 3900 clones from the tail library and a summary of the screening outcome is presented in Table 1. In stage two of the screen, only 9 out of 100 clones selected from the ring library were active when culture supernatants were applied on susceptible *S. Newport*. In contrast, 57 out of the 67 clones tested against *S. Newport* in the tail library



**Figure 4.** Representation of relative zone of inhibition diameter for all sequenced ring (red), tail (green), and tail ara+ (blue) library variants normalized to wild type MccJ25 zone diameter in *S. Newport* growth inhibition assay. Only a few functional ring library variants were isolated from the screen, and the variants have much smaller inhibition zone diameter compared with wild type. Overall the tail library variants have much larger inhibition zone diameters. In the tail ara+ library, only clones exhibiting relative zone diameter >0.80 were sequenced and shown here. Inset: Histogram representation plotting the total number of sequenced variants in the ring, tail, or tail ara+ libraries at various relative zone diameter levels.

displayed antibacterial activity. We note that over half of the clones from stage one in both the ring and tail library were growth inhibited to some degree on the IPTG/glucose plate (Supplementary Figure 1), indicating that both libraries contain a substantial number of variants that were matured into the lasso fold and capable of intracellular action against RNAP or the respiratory chain. These results point to the conclusion that multiple substitutions to either the ring or tail portion of the peptide are tolerated for intracellular antimicrobial activity. However, while substitutions in the tail region were tolerated for cell entry, the ring library variants were frequently incapable of being transported into the cytoplasm of the susceptible strains. To confirm that we were not simply observing false positives in stage one of the ring library screen, several of the clones from stage one were grown in liquid media and spotted on plates either containing arabinose or glucose/IPTG. All variants grew normally on the arabinose plate, but most of the variants were growth inhibited on glucose/IPTG (Supplementary Figure 2).

We measured the diameter of all inhibition zones against *S. Newport* from the stage two screening to provide a quantitative preliminary indicator of the activity of the MccJ25 variants from the libraries. The ratio of the variant zone diameter to wild type MccJ25 zone diameter was determined as the relative zone diameter (Figure 4, Supplementary Table 2). An alternative binned histogram view of this data is presented as the inset in Figure 4. It should be noted that the inhibition zone diameter does not vary linearly with increasing efficacy of the antibiotic. For example, in our previous work,<sup>38</sup> we found that a 1.5-fold increase in *S. Newport* inhibition zone diameter corresponds to a

16-fold increase in MccJ25 titer. Among the eight distinct clones from the ring library that killed *S. Newport*, all displayed much smaller inhibition zone diameter than that of wild-type MccJ25 (Figure 4). Moreover, six of the eight sequences only have two aa substitutions (Supplementary Table 2). The activity of variants from the tail library against *S. Newport* are much higher on average and ranged from weak to wild-type level based on the inhibition zone diameter (Figure 4). From these data, we can conclude that the aa sequence of MccJ25 is much more tolerant to multiple substitutions in the tail region than the ring region in retaining the overall function of the peptide.

Since the tail library was more amenable to substitutions, we further screened this library in an attempt to discover MccJ25 variants with improved efficacy toward either *S. Newport* or *E. coli* DH5 $\alpha$ . We hypothesized that leaky expression of highly active variants could potentially poison cells harboring such variants if MccJ25 was not produced. In this scenario, cells expressing the most potent variants would not survive the initial transformation step of library creation. To circumvent this limitation, we repeated the library transformation and screening keeping arabinose present at all times to induce MccJ25 expression except during the transfer of colonies on the IPTG/glucose plates. As it was possible that some arabinose was carried over onto the IPTG/glucose plates during replica plating, we found mostly clones that were weaker in growth but not completely inhibited. Clones that appeared to be strongly growth inhibited on the plates were selected for supernatant testing by the zone of inhibition assay. Of the 247 clones selected for stage two screening from this tail ara+ library, 193 clones had activity against *S. Newport*, among which 43 had large inhibition zone diameter (Table 1). For the tail ara+ library, only variants with large inhibition zone were sequenced and the zone diameter of the sequenced clones is shown in Figure 4. Several variants had relative zone diameter of greater than 1. Since the results from this antimicrobial activity assay depended on the amount of MccJ25 derivatives in the crude supernatants, highly active antibacterial derivatives from the tail and tail ara+ libraries were further characterized to determine their efficacy.

**Efficacy and Production Level of the Variants.** The antimicrobial activity of MccJ25 variants from the tail and tail ara+ library that had relative zone inhibition diameter above a cutoff of 0.8 was directly assessed by determining their last active dilution (LAD). The LAD for each variant was determined as the last dilution of supernatant that resulted in growth inhibition on a lawn of susceptible organism. This analysis was performed on both *S. Newport* and *E. coli* DH5 $\alpha$ . The amount of the MccJ25 derivatives in the supernatants was determined by applying supernatant extracts to analytical HPLC and integrating the area under the peak as we have previously described.<sup>34,38</sup> The relative production level of these variants ranged from about 0.5- to 2-fold of the production level of wild-type MccJ25. The relative efficacy of the variants (Table 2) takes into account both the dilution analysis and the production level of the variants. Relative efficacy was calculated by taking the ratio of the LAD of the variant and the LAD of wild-type MccJ25 and normalizing this value by the relative production level of the variant as determined by HPLC. One limitation of using a zone of inhibition diameter cutoff of 0.8 is the potential to miss highly potent but poorly expressed MccJ25 variants. To control for this possibility, we measured the zone of inhibition and relative production level of an unbiased set of 17 functional mutants from the tail ara+ library. The production level of these variants ranged from 0.25- to 2.3-fold of the wild-type MccJ25 production level (Supplementary Table 2). It should be noted that there was only a single variant with a relative production level of 0.25 and it had a correspondingly small zone of



Table 2. Sequences of MccJ25 Tail Library Variants with Relative Efficacy Exceeding Wild Type MccJ25

MccJ25 variant	residues			last active dilution <i>S. Newport</i> <sup>a</sup>	last active dilution <i>E. coli</i> DH5 $\alpha$ <sup>a</sup>	HPLC retention time (min)	relative production level from HPLC <sup>b</sup>	relative efficacy <i>S. Newport</i> <sup>c</sup>	relative efficacy <i>E. coli</i> <sup>c</sup>
WT	Gly-12	Ile-13	Thr-15	512	4	16.0	1	1	1
Tail									
15	Thr	Leu	Ile	512	8	18.1	0.88	1.1	2.3
39	Phe	His	Val	256	8	16.4	1.0	0.50	2.0
Tail ara+									
33	Phe	Pro	\	512	8	17.3	0.79	1.3	2.5
34	Ala	Leu	\	256	8	16.7	1.0	0.50	2.0
49	His	Tyr	Ile	512	8	15.8	0.5	2.0	4.0
53	His	Phe	Ile	1024	8	17.4	0.42	4.8	4.8
56	Ser	Ala	Phe	256	4	16.1	0.75	0.67	1.3
59	\	Pro	Phe	512	8	16.6	0.65	1.5	3.1
140	Ala	\	\	256	16	16.5	1.0	0.50	4.0
146	His	Leu	Ala	256	8	16.2	0.77	0.65	2.6
211	His	Leu	Val	1024	8	16.5	0.51	3.9	3.9
217	Ala	Leu	Ala	256	8	16.9	1.2	0.42	1.7

<sup>a</sup> Last serial dilution of culture supernatant resulting in growth inhibition in plate assays, each measurement was repeated at least three times. <sup>b</sup> HPLC peak areas of variants were normalized by the HPLC peak area of wild-type MccJ25. <sup>c</sup> Last active dilution (LAD) values of variants were first normalized by the LAD of wild-type MccJ25 and then normalized by relative production level.

inhibition. From this survey of an unbiased set of MccJ25 variants, we conclude that the production level of most functional MccJ25 variants in the tail ara+ library lies in a relatively small range of ~0.5- to ~2-fold of the wild-type production level.

The 12 distinct variants that had improved relative efficacy against *E. coli* DH5 $\alpha$  or *S. Newport* are listed in Table 2. Of these 12 variants, 6 displayed improved efficacy against *S. Newport*. The variants with the highest activity against *S. Newport*, clones 53 and 211 from the tail ara+ library, showed a relative LAD 2-fold higher than wild-type and the relative production level was 0.42 and 0.51, resulting in a relative efficacy 4.8- and 3.9-fold higher than wild type MccJ25, respectively. All 12 variants also exhibited improved antimicrobial activity against the *E. coli* strain DH5 $\alpha$  with three of the variants (tail ara+ 49, 53, and 140) exhibiting relative efficacies of 4-fold or greater (Table 2). These variants produced markedly clear inhibition zones against *E. coli*, unlike the turbid zone produced by wild type MccJ25 (Supplementary Figure 4). It is noteworthy that variants with improved activity against *E. coli* do not always have improved activity against *S. Newport*. However, each of the six variants with improved efficacy against *S. Newport* show improved efficacy against *E. coli* too (Table 2).

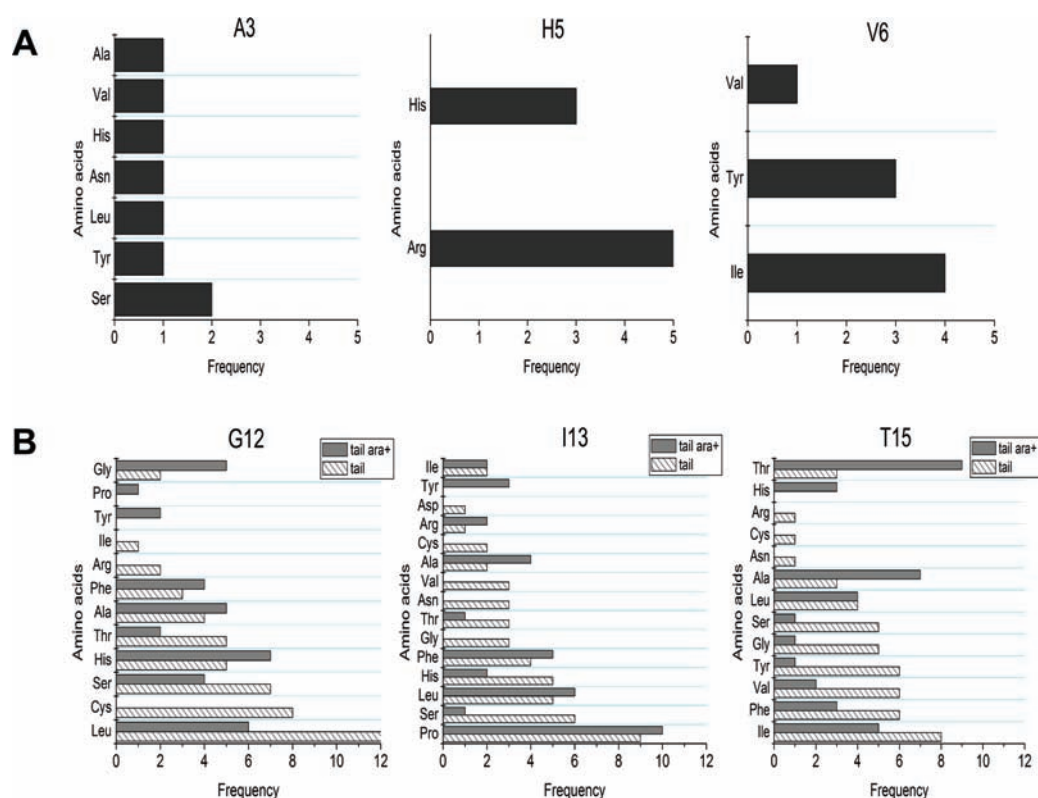
**Sequences of the Variants.** Among the variants with improved efficacy toward *S. Newport* (tail 15; tail ara+ 33, 49, 53, 59, 211), position Gly-12 was most frequently substituted by His, Ile-13 by Leu and Pro, and Thr-15 by Ile (Table 2). As mentioned above, all of the variants in Table 2 have higher activity against *E. coli* DH5 $\alpha$ . Among these variants, Gly-12 was most frequently substituted by either Ala or His, and Ile-13 was substituted by Leu and Pro. Thr-15 was not substituted in three of the variants exhibiting improved activity toward *E. coli*. Beneficial substitutions at Thr-15 included Ala and Ile. Thus, while the G12H, I13L, I13P, and T15I substitutions were found to be beneficial to both *Salmonella* and *E. coli* growth inhibition, the G12A and T15A substitutions appeared to be beneficial only for *E. coli* inhibition.

A breakdown of the amino acid substitutions of all of the distinct sequences from the ring library (8 sequences), tail library (49 sequences), and tail ara+ library (36 sequences, Table 1) are

shown in Figure 5. The sequences of each of these distinct variants are given in Supplementary Table 3. It should be noted that while all functional variants from the tail library were sequenced, only those variants exhibiting high activity (as evidenced by a large zone of growth inhibition in the spot-on-lawn assay) were sequenced from the tail ara+ library. Among the ring library variants (Figure 5A), a range of substitutions to the Ala-3 position were tolerated with no specific aa preference; His-5 was only replaced by Arg, and Val-6 was replaced by Ile and Tyr. For the tail variants (Figure 5B), a wide variety of aa substitutions could be found in any of the three positions. Position 13 was especially flexible and could tolerate any of the 15 residues represented by the NNT codon.

## DISCUSSION

We constructed mutagenesis libraries with site-directed substitutions at three aa positions in the ring (A3, H5, V6) or tail (G12, I13, T15) region of MccJ25. We found that a large proportion (roughly half, see Supplementary Figure 1) of the members from both the ring and tail libraries retain some intracellular antimicrobial activity, providing evidence that the threaded lasso structure of MccJ25 is retained even upon multiple aa substitutions. The most potent MccJ25 variants from the tail library displayed up to a nearly 5-fold improvement in bacterial growth inhibition action against *E. coli* DH5 $\alpha$  and/or *S. Newport*. It is noteworthy that, although MccJ25 demonstrates exceptional potency against the sensitive strain *S. Newport* with minimal inhibitory concentration (MIC) in the range of ~10 nM,<sup>26,32</sup> variants with up to 4.8-fold greater potency were still discovered. The degree of improvement in activity against the two different strains often differs; generally, variants with improved activity against *E. coli* are more likely to be found than those against *S. Newport* in the tail library (Table 2). The substitutions beneficial to the killing function of MccJ25 tend to be hydrophobic amino acids with the exception of the G12H substitution. Since the killing of bacteria by MccJ25 comes about via multiple biomolecular interactions, it is difficult to pinpoint the reason for the increased potency of the MccJ25 variants in Table 2. These variants may exhibit increased



**Figure 5.** Amino acid substitutions observed in functional variants of MccJ25. The frequency unit on the *x*-axis is the number of times a given substitution appeared among sequenced library variants. (A) Only several aa substitutions in each position in the ring portion of the peptide were tolerated. (B) In contrast, the tail portion of the peptide was much more amenable to substitutions in all positions mutagenized in the tail and tail ara+ libraries. Amino acid sequences of each of the individual variants are given in Supplementary Table 2.

potency because of improved interactions with the import proteins FhuA and SbmA or the antimicrobial target RNAP. An alternative possibility is that wild-type MccJ25 is a substrate for an intracellular protease, and the aa substitutions in the potent variants stabilize the peptide against such a protease. There is some precedence for intracellular proteases protecting cells against antimicrobial peptides. For example, it has been inferred that the periplasmic protease DegP degrades the antimicrobial peptide lactoferrin.<sup>39</sup>

Pavlova et al.<sup>15</sup> reported that, aside from the Gly-1 and Glu-8 residues necessary to form the lactam macrocycle, the glycine residues at positions 2 and 4 and the proline residue at position 7 are strictly essential for bacterial growth inhibition. The ring library results presented in this work confirm that substitutions at the remaining positions of the ring are also extremely deleterious to antibacterial action. However, we also demonstrate here that many of the ring library variants are functional in the cytoplasm of *E. coli*, indicating that variations in the ring sequence likely disrupt import of MccJ25 to the cytoplasm. Thus, MccJ25 import appears to have a stringent requirement for the residues in the ring and the native sequence may be well-optimized for this function. In contrast, positions 12, 13, and 15 in the tail region are permissive to substitutions while retaining antimicrobial activity. Collectively, this data allows us to expand upon the current structure–activity relationship data on MccJ25. While it has been previously demonstrated that His-5 plays an important role in the SbmA-mediated transport of MccJ25 into the cytoplasm of susceptible cells,<sup>31</sup> we show here that other variations in the ring sequence are also deleterious for MccJ25 import. Furthermore, while previous studies demonstrated that cleavage of the  $\beta$ -hairpin region of the tail abrogated import of MccJ25 by disruption of its interaction

with FhuA, we show that multiple concurrent amino acid substitutions can be tolerated in this region of the peptide without loss of recognition by FhuA.

In the Pavlova et al. study,<sup>15</sup> singly substituted variants of MccJ25 were all tested for production, maturation and export. Compatible substitutions were next assessed for inhibition of RNAP. Lastly, substitutions compatible with both production and RNAP inhibition were assessed for inhibition of bacterial growth. The functional variants from our libraries frequently contain substitutions that were found to be not tolerated in the study, at all levels of assessment: inhibition of bacterial growth, RNAP inhibition, and even production/maturation/export. Several explanations could account for this observation. The effects of the nontolerated substitution can be compensated by the other substitutions in the variant. The variant may exert its cytoplasmic action on the respiratory chain target instead of RNAP. We also note that the *S. Newport* strain used in our screening for susceptibility testing is much more sensitive than the *E. coli* or *Shigella* strains used by Pavlova et al. and therefore may capture variants with antibacterial activity below the threshold for detection in their study. Among the variants with the highest activity, the majority of substitutions we observe at G12 and I13 are tolerated single aa substitutions in the Pavlova et al. study, with the exception of G12F and I13Y. At position 15, Thr is frequently substituted by Val or Ile, which are not tolerated even at the level of production or RNAP inhibition, respectively, as single substitutions.

Other known members of the class II lasso peptides, which form a lactam bond between the N-terminus glycine and either a glutamic acid or aspartic acid side chain, include capistrin produced by a *Burkholderia* strain that exhibits antimicrobial activity against closely

related strains,<sup>12,13</sup> the antimycobacterial peptide lariatin,<sup>11</sup> and the endothelin B receptor selective antagonist RES-701-1.<sup>10</sup> There is little sequence similarity among these peptides except for the conserved glycine and glutamic acid or aspartic acid required for cyclization. In the absence of clear sequence trends in known examples of lasso peptides, the screening approach presented here can provide information about the extent of sequence space permitting maturation and folding of lasso peptides. Our results indicate that the sequence space that lasso peptides occupy is quite extensive. Given the extraordinary resistance of lasso peptides to proteases and thermal unfolding and the ability to program diverse sequences into the lasso framework, lasso peptides appear to be a promising platform for therapeutic peptide applications.

## ■ ASSOCIATED CONTENT

**S Supporting Information.** Examples of replica plates, zone of inhibition plate assay, table of sequences and zone diameter of MccJ25 variants, table of plasmids and primers. This material is available free of charge via the Internet at <http://pubs.acs.org>.

## ■ AUTHOR INFORMATION

**Corresponding Author**  
ajlink@princeton.edu

## ■ ACKNOWLEDGMENT

The authors thank Wai Ling Cheung for the construction of the pWC8 plasmid. This work was supported by Princeton University startup funds and by an NSF CAREER grant (Grant No. CBET-0952875).

## ■ REFERENCES

- (1) Severinov, K.; Semenova, E.; Kazakov, A.; Kazakov, T.; Gelfand, M. S. *Mol. Microbiol.* **2007**, *65*, 1380.
- (2) Duquesne, S.; Petit, V.; Peduzzi, J.; Rebuffat, S. *J. Mol. Microbiol. Biotechnol.* **2007**, *13*, 200.
- (3) Baquero, F.; Moreno, F. *FEMS Microbiol. Lett.* **1984**, *23*, 117.
- (4) Duquesne, S.; Destoumieux-Garzon, D.; Peduzzi, J.; Rebuffat, S. *Nat. Prod. Rep.* **2007**, *24*, 708.
- (5) Pavlova, O. A.; Severinov, K. V. *Russ. J. Genet.* **2006**, *42*, 1380.
- (6) Bayro, M. J.; Mukhopadhyay, J.; Swapna, G. V. T.; Huang, J. Y.; Ma, L. C.; Sineva, E.; Dawson, P. E.; Montelione, G. T.; Ebright, R. H. *J. Am. Chem. Soc.* **2003**, *125*, 12382.
- (7) Rosengren, K. J.; Clark, R. J.; Daly, N. L.; Goransson, U.; Jones, A.; Craik, D. J. *J. Am. Chem. Soc.* **2003**, *125*, 12464.
- (8) Wilson, K. A.; Kalkum, M.; Ottesen, J.; Yuzenkova, J.; Chait, B. T.; Landick, R.; Muir, T.; Severinov, K.; Darst, S. A. *J. Am. Chem. Soc.* **2003**, *125*, 12475.
- (9) Rebuffat, S.; Blond, A.; Destoumieux-Garzon, D.; Goulard, C.; Peduzzi, J. *Curr. Prot. Pept. Sci.* **2004**, *5*, 383.
- (10) Katahira, R.; Shibata, K.; Yamasaki, M.; Matsuda, Y.; Yoshida, M. *Bioorg. Med. Chem.* **1995**, *3*, 1273.
- (11) Iwatsuki, M.; Tomoda, H.; Uchida, R.; Gouda, H.; Hirono, S.; Omura, S. *J. Am. Chem. Soc.* **2006**, *128*, 7486.
- (12) Knappe, T. A.; Linne, U.; Zirah, S.; Rebuffat, S.; Xie, X. L.; Marahiel, M. A. *J. Am. Chem. Soc.* **2008**, *130*, 11446.
- (13) Knappe, T. A.; Linne, U.; Robbel, L.; Marahiel, M. A. *Chem. Biol.* **2009**, *16*, 1290.
- (14) Everts, S. *Chem. Eng. News* **2010**, *88*, 38.
- (15) Pavlova, O.; Mukhopadhyay, J.; Sineva, E.; Ebright, R. H.; Severinov, K. *J. Biol. Chem.* **2008**, *283*, 25589.

- (16) Pan, S. J.; Cheung, W. L.; Fung, H. K.; Floudas, C. A.; Link, A. J. *Protein Eng., Des. Sel.* **2010**, *24*, 275.
- (17) Delgado, M. A.; Rintoul, M. R.; Farias, R. N.; Salomon, R. A. *J. Bacteriol.* **2001**, *183*, 4543.
- (18) Yuzenkova, J.; Delgado, M.; Nechaev, S.; Savalia, D.; Epshtein, V.; Artsimovitch, I.; Mooney, R. A.; Landick, R.; Farias, R. N.; Salomon, R.; Severinov, K. *J. Biol. Chem.* **2002**, *277*, 50867.
- (19) Mukhopadhyay, J.; Sineva, E.; Knight, J.; Levy, R. M.; Ebright, R. H. *Mol. Cell* **2004**, *14*, 739.
- (20) Adelman, K.; Yuzenkova, J.; La Porta, A.; Zenkin, N.; Lee, J.; Lis, J. T.; Borukhov, S.; Wang, M. D.; Severinov, K. *Mol. Cell* **2004**, *14*, 753.
- (21) Rintoul, M. R.; de Arcuri, B. F.; Salomon, R. A.; Farias, R. N.; Morero, R. D. *FEMS Microbiol. Lett.* **2001**, *204*, 265.
- (22) Bellomio, A.; Vincent, P. A.; de Arcuri, B. F.; Farias, R. N.; Morero, R. D. *J. Bacteriol.* **2007**, *189*, 4180.
- (23) Salomon, R. A.; Farias, R. N. *J. Bacteriol.* **1993**, *175*, 7741.
- (24) Salomon, R. A.; Farias, R. N. *J. Bacteriol.* **1995**, *177*, 3323.
- (25) Semenova, E.; Yuzenkova, Y.; Peduzzi, J.; Rebuffat, S.; Severinov, K. *J. Bacteriol.* **2005**, *187*, 3859.
- (26) Bellomio, A.; Vincent, P. A.; de Arcuri, B. F.; Salomon, R. A.; Morero, R. D.; Farias, R. N. *Biochem. Biophys. Res. Commun.* **2004**, *325*, 1454.
- (27) Destoumieux-Garzon, D.; Duquesne, S.; Peduzzi, J.; Goulard, C.; Desmadril, M.; Letellier, L.; Rebuffat, S.; Boulanger, P. *Biochem. J.* **2005**, *389*, 869.
- (28) Socias, S. B.; Severinov, K.; Salomon, R. A. *FEMS Microbiol. Lett.* **2009**, *301*, 124.
- (29) Rosengren, K. J.; Blond, A.; Afonso, C.; Tabet, J. C.; Rebuffat, S.; Craik, D. J. *Biochemistry* **2004**, *43*, 4696.
- (30) Vincent, P. A.; Bellomio, A.; de Arcuri, B. F.; Farias, R. N.; Morero, R. D. *Biochem. Biophys. Res. Commun.* **2005**, *331*, 549.
- (31) de Cristobal, R. E.; Solbiati, J. O.; Zenoff, A. M.; Vincent, P. A.; Salomon, R. A.; Yuzenkova, J.; Severinov, K.; Farias, R. N. *J. Bacteriol.* **2006**, *188*, 3324.
- (32) Salomon, R. A.; Farias, R. N. *J. Bacteriol.* **1992**, *174*, 7428.
- (33) Solbiati, J. O.; Ciaccio, M.; Farias, R. N.; Gonzalez-Pastor, J. E.; Moreno, F.; Salomon, R. A. *J. Bacteriol.* **1999**, *181*, 2659.
- (34) Pan, S. J.; Cheung, W. L.; Link, A. J. *Protein Expression Purif.* **2010**, *71*, 200.
- (35) Duquesne, S.; Destoumieux-Garzon, D.; Zirah, S.; Goulard, C.; Peduzzi, J.; Rebuffat, S. *Chem. Biol.* **2007**, *14*, 793.
- (36) Solbiati, J. O.; Ciaccio, M.; Farias, R. N.; Salomon, R. A. *J. Bacteriol.* **1996**, *178*, 3661.
- (37) Guzman, L. M.; Belin, D.; Carson, M. J.; Beckwith, J. *J. Bacteriol.* **1995**, *177*, 4121.
- (38) Cheung, W. L.; Pan, S. J.; Link, A. J. *J. Am. Chem. Soc.* **2010**, *132*, 2514.
- (39) Ulvatne, H.; Haukland, H. H.; Samuelsen, O.; Kramer, M.; Vorland, L. H. *J. Antimicrob. Chemother.* **2002**, *50*, 461.